Reduction of effective material loss (EML) using decagonal photonic crystal fiber (D-PCF) for communication applications in the terahertz wave pulse

Selim Hossain
Daffodil International University
Shuvo Sen (shuvombstu.it12009@gmail.com)
Mawlana Bhashani Science and Technology University

Research Article

Keywords: Low loss EML, Confinement Loss, Effective Area, Scattering Loss, Optical Communication.

Posted Date: May 12th, 2022

DOI: https://doi.org/10.21203/rs.3.rs-1400148/v1

Reduction of effective material loss (EML) using decagonal photonic crystal fiber (D-PCF) for communication applications in the terahertz wave pulse

Md. Selim Hossain[1], Shuvo Sen[2*]

[1]Department of Computing and Information System, Daffodil International University, Dhaka, Bangladesh

[2] Department of Information and Communication Technology (ICT), Mawlana Bhashani Science and Technology University (MBSTU), Santosh, Tangail-1902, Bangladesh

*Corresponding Author: Mawlana Bhashani Science and Technology University, Santosh, Tangail-1902, Bangladesh

Email: shuvombstu.it12009@gmail.com

Abstract

We present an excellent design of five layers of decagonal shape in the cladding area and two elliptical shapes of core area based photonic crystal fiber (PCF) for many types of communiqué arenas in the THz wave pulse in this study. The Finite Element (FEM) method with perfectly matched layers (PML) used the optical parameters of our proposed D-PCF structure numerically to design and analyze. Therefore, D-PCF shows a low effective material loss (EML) of 0.0079 cm^{-1}, an increase in effective area (EA) of 3.49×10^{-8} m^2, a core power fraction of 85%, a low confinement and scattering loss, such as3.35×10^{-16} dB/m and 1.27×10^{-10} dB/km respectively at 1 THz of frequency respectively. After analyses all the graphical results, our proposed D-PCF will be highly suitable for communiqué parts in the THz regions.

Keywords: Low loss EML, Confinement Loss, Effective Area, Scattering Loss, Optical Communication.

Introduction

Terahertz radiation which ranges from 0.1 to 10 THz, has recently sparked considerable interest due to its many applied submissions. The gray area exists within the situation of ultraviolet radioactivity and the microwave range. The huge THz occurrence has applications in a variety of fields such as detection [1-2], biomedical tomography [3], transport network [4], bioengineering [5], time-domain spectrometry [6], brininess [7], infection sensor [8], security screening [9] applications. It also makes significant advances in the roots and documentation systems of the THz wave. The whole THz scheme is made up of three distinct parts: THz sources, wave

guidance, and sensors. THz detector are commercially accessible. THz foundations and sensors are being quickly promoted with the help of advanced up-to-date expertise. The most important THz sources are Gunn diodes, free-electron lasers, quantum lasers, biological gas far-infrared lasers, and so on. Furthermore, the most useful T-ray detectors are bolometers, Golay cells, pyroelectric detectors, and Schottky barrier diodes. Most THz waveguides, however, rely heavily on free-space wave proliferation due to frequency propagation. However, here are some issues with free space wave proliferation, such as path loss, material loss, and high absorption loss. Researchers had previously proposed numerous waveguides to mitigate these issues. Bragg fibers [13], metallic waveguides [10], silver coated hollow glass [11-12], subwavelength waveguides [14], parallel-plate waveguides [15], and so on are examples. Metallic waveguides used in THz transmission can encounter issues such as high winding loss and frequency-dependent losses. Bragg fibers are more efficient in diffusion and riddling submissions. Nonetheless, using Bragg fibers to achieve desirable output in applied wavelength division multiplexing submissions is difficult. The main limitation of a parallel-plate waveguide is confinement loss.

Microstructure core PCF has newly demonstrated progressive physical elasticity and extremely high optical possessions. One important gain is that determined optical power permits through the core region, which aids to decrease material loss. Two basic optical managerial possessions are usually originated in microstructure core PCF: modified total internal reflection (MTIR) and photonic bandgap (PBG). When the RI of the cladding is better than the core RI, the photonic bandgap function operates in PCF. When the core RI exceeds the cladding, the MTIR impact is activated. Microstructure PCF is proposed as a THz supervisory standard to attain lower confinement loss, high numerical aperture, lower dispersion, high birefringence, and better waveguiding properties. PCF suffers from material losses due to the use of solid materials in the core region. A porous air core is favored athwart a solid body [16]. Such properties make it possible to use porous polymer PCFs in a variety of filtering and sensing submissions. Other kinds of circumstantial resources, such as ZEONEX, TOPAS, Teflon, Polymethyl methacrylate, and ZBLAN [17-21], are secondhand to improve optical guiding properties and reduce EML. ZEONEX has been used as the contextual material since it has excellent optical possessions such as low material loss, high temperature insensitivity, and low dispersion [22].

In past years, low loss THz waveguides are discussed briefly by many researchers. Porous core-based PCF was described by Hasanuzzaman et al. [23] and presented the higher effective EML of 0.035 cm^{-1}. Hasan et al. [24] discussed a square lattice photonic crystal fiber and reported an EML of 0.076 cm^{-1}. Islam et al. [25] showed their structure such as porous core-based PCF and found an EML of 0.050 cm^{-1}. Sen et al. [26] showed the polymer-based photonic crystal fiber and their results of an EML of 0.040 cm^{-1}. After checking the previous structure [23-26], we get a good chance to develop a new structure by removing very low losses for communication applications.

Our D-PCF is an arrangement of five layers of decagonal form within the covering area and two elliptical forms of photonically crystal (D-PCF) core area of various types of communication in the terahertz belt. This D-PCF displays a low EML of 0,0079 cm^{-1} following an examination of numerical findings; a large effective area of 3.49×10^{-8} m^2; a core power fraction (CPF) of 85%, a low CL and SL of as 3.35×10^{-16} dB/m and 1.27×10^{-10} dB/km at 1 THz respectively.

Design Methodology of D-PCF

Figure 1 depicts structural cross sections such as (a) Decagonal cladding regions, (b) Elliptical core regions, and (c) Mode field distribution. In this case, the diameter and pitch at the cladding areas are signified by the constraints d_1 and A_1. The constraints d_1/A_1 is called the air filling proportion which is to watch in contradiction of collapse between two air holes in the cladding area. The parameters of A_c, d_a, and d_b are indicated at the core area by the pitch and distances of the two elliptical AHs. The ZEONEX material was used to remove the EML, confinement loss (CL), and Scattering loss (SL) in this case. Here, the optimum cladding diameter is 282 μm, cladding pitch of 345 μm, diameter of core d_a = 70 μm, d_b= 160 μm and core pitch Λ_c=100 μm.

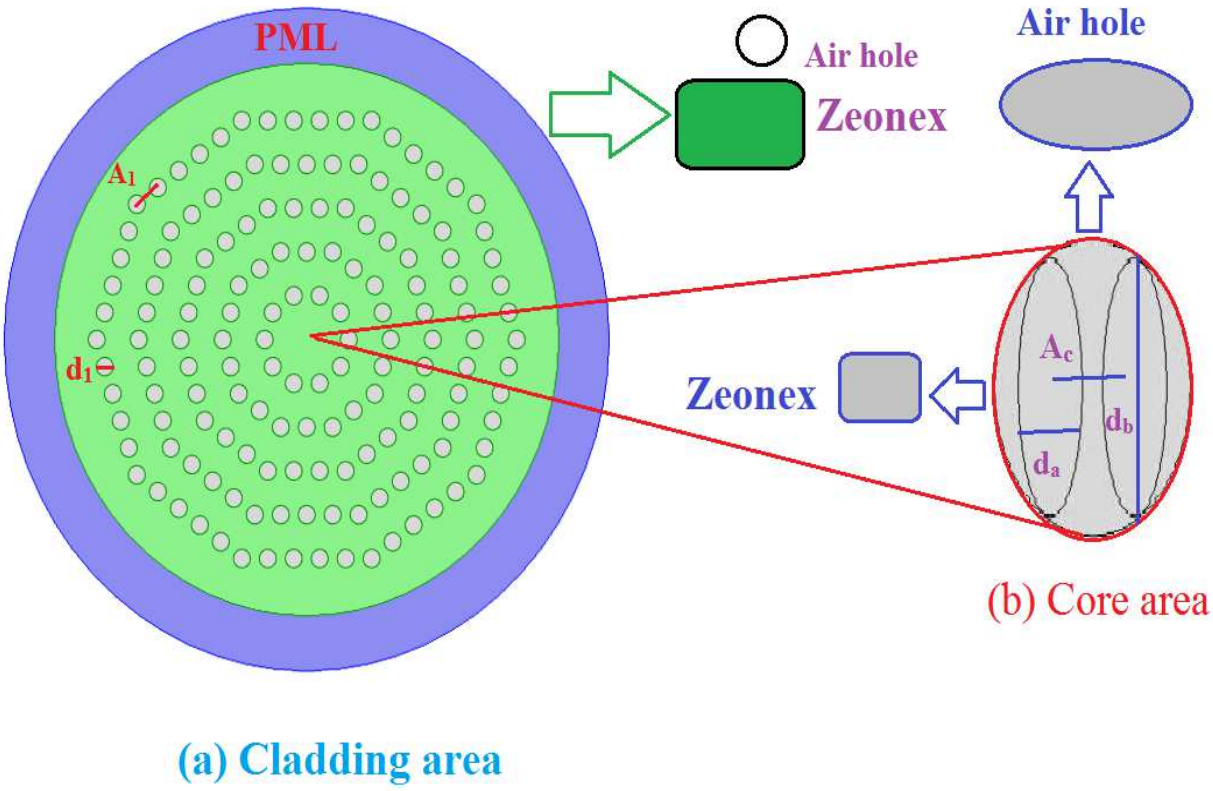

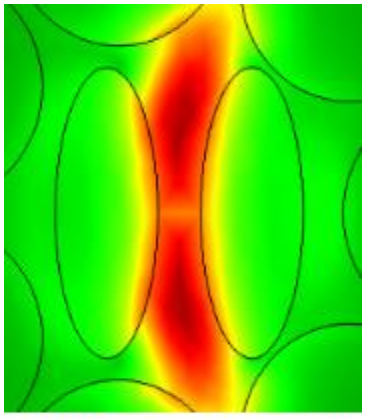

(c) Mode field distribution

Figure 1: Designed sights of D-PCF fiber, (a) Cladding area (b) Elliptical core area (c) Mode field distributions for both x and y polarization at the frequency of 1 THz.

Mathematical Analysis of Optical Properties:

It has been known to us that a large EA-based PCF fiber shows a low EML. Here, the EA is calculated the following equation [27]:

$$A_{ea} = \frac{[\int I(e)ede]^2}{[\int I^2(e)de]^2} \quad (1)$$

Where, A_{ea} is the effective area and intensity electric field is the $I(e) = |E_e|^2$

PF is indicated that the most amount of power flowing in the core area of the D-PCF structure. Here, Power fraction is determined by the equation [28]:

$$\eta = \frac{\int_i S_{zt} dAt}{\int_{all} S_{zt} dAt} \quad (2)$$

V-parameter displays the single mood communication and the V-parameter is shown the following equation [29]:

$$V = \frac{2\pi ef}{c} \sqrt{ne^2_{coe} - ne^2_{cle}} \leq 2.045 \quad (3)$$

Where, the core and cladding area based effective mood index is defined by the n_{coe} and n_{cle} and c is the radius of the core.

The CL is a vital aspect of D-PCF structure and this CL (L_{ce}) is shown by [30]:

$$L_{ce} = 8.686 \times K_0 \, Im\,[n_{ea}] \ (dB/m) \quad (4)$$

Where, the free wave number is $K_0 = \left(\frac{f}{c}\right)$, c is the speed of photon, frequency is f and the imaginary part of ERI is $Im\,[n_{ea}]$.

The SL is well-defined with the total amount of loss of the D-PCF structure. At this time, the scattering loss is calculated by [31]:

$$\alpha_S = C_S \times \left(\frac{f}{c}\right)^4 (dB/km) \quad (5)$$

Where, the scattering coefficient is C_S .

The background material of Zeonex creates a very low EML and this EML is calculated by [32]:

$$\alpha_{ea} = \sqrt{\frac{\varepsilon_0}{\mu_0}} \left(\frac{\int_{mat} n_{mat} |E|^2 \alpha_{mat} \, dAt}{|\int_{all} S_{zt} dAt|}\right) (cm^{-1}) \quad (6)$$

Simulated Results and Discussions:

We chose the optimum porosity of 86 percent, 76 percent, and 66 percent because it is clear from Figures 2 to 9 that the total light transmits inside the CA. This D-PCF fiber exhibits improved graphic outputs for optical possessions such as low EML, low SL, larger EA, high core power fraction, better V-parameter, and low CL with frequency ranges ranging from 0.08 to 3 THz.

In Figure 2, the EA is decreasing with the frequency varieties from 0.80 to 3 THz for three porosities for such as 66%, 76%, and 86%. At 1 THz frequency of optimum parameters for 86%, 76%, and 66% porosities, the EA is determined of 3.49×10^{-8} m^2, 3.60×10^{-8} m^2, and 4.55×10^{-8} m^2.

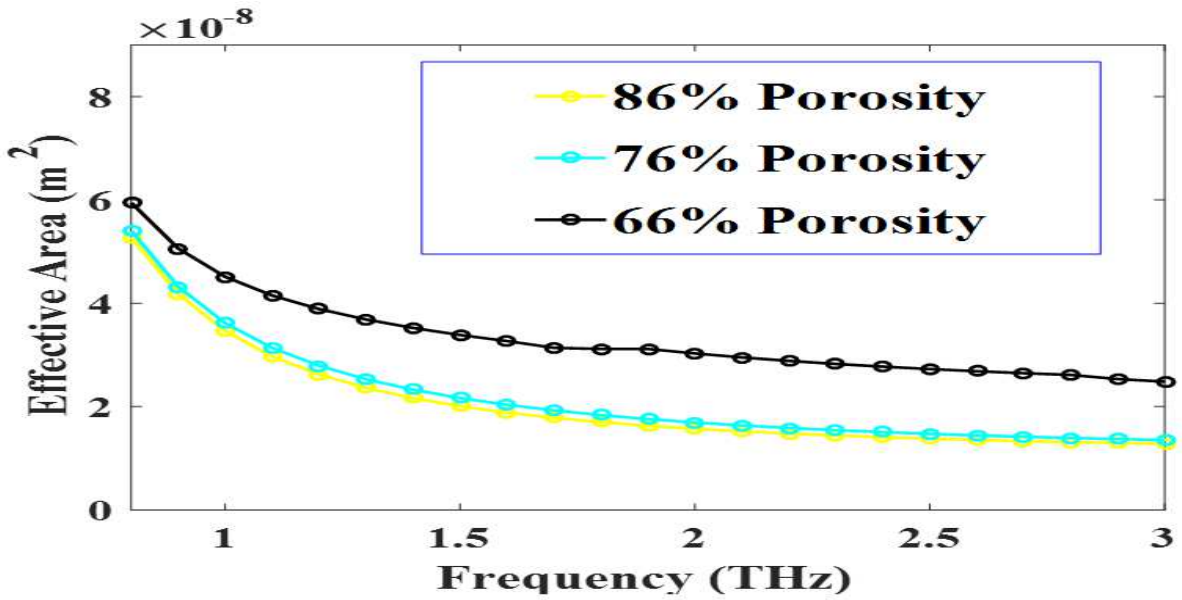

Figure 2: Calculation of EA along with the frequencies.

Here, EA is slightly decreased with the core diameters from D_{core} = 280 µm to D_{core} = 440 µm for three porosities for such as 66%, 76%, and 86% in Figure 3. At 1 THz frequency of optimum parameters for 86%, 76%, and 66% porosities, the EA is determined as 4.27×10^{-8} m^2, 4.55×10^{-8} m^2, and 4.63×10^{-8} m^2.

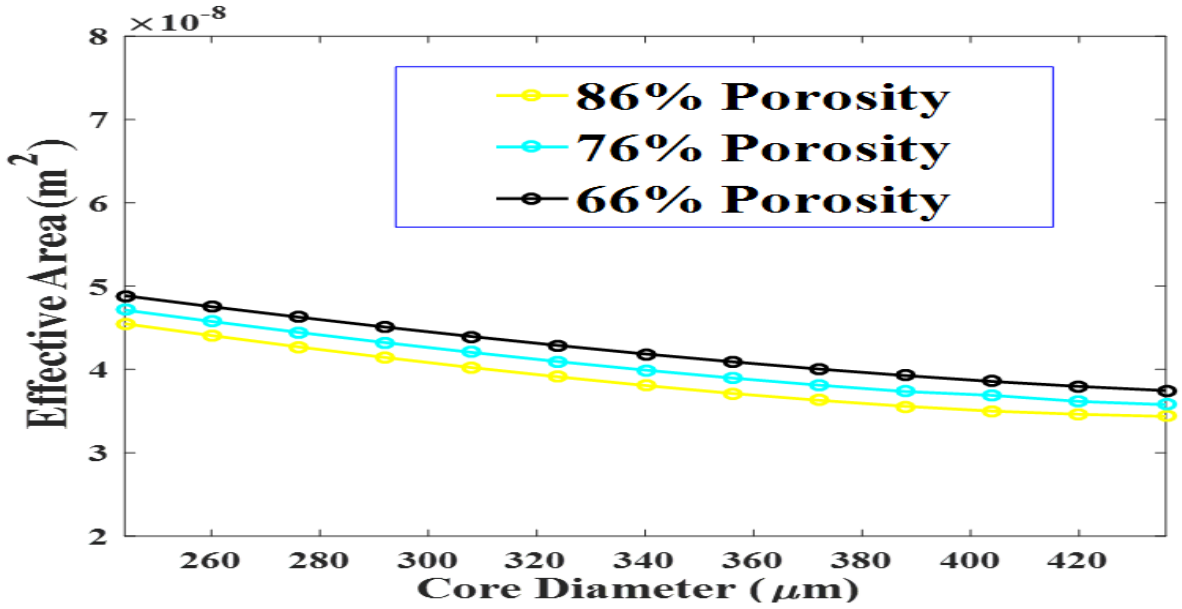

Figure 3: Calculation of in accordance with the core diameters.

In Figure 4, the EML is a very decreasing with the frequency assortments from 0.80 to 3 THz for three porosities for such as 66%, 76%, and 86%. At 1 THz frequency of optimum parameters for 86%, 76%, and 66% porosities, the EML is measurement of 0.0079 cm^{-1}, 0.0069 cm^{-1} and 0.0127 cm^{-1}.

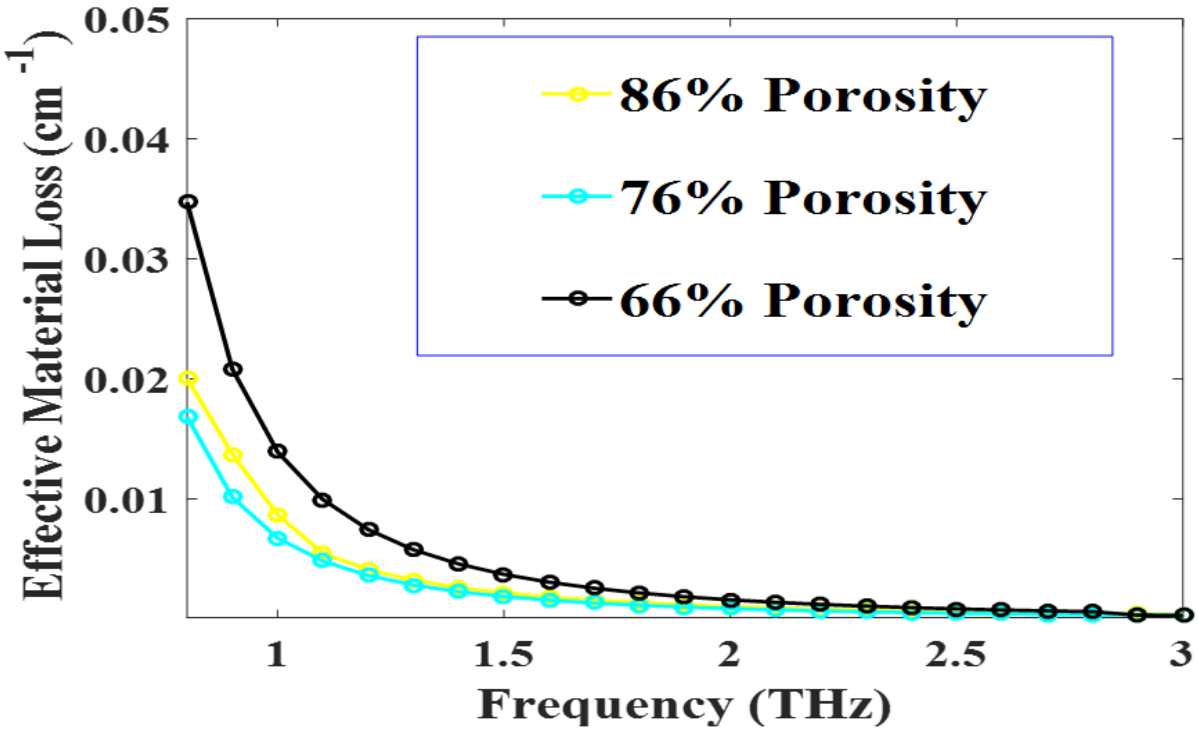

Figure 4: Measurement of EML with respect to the frequencies.

In these graphical results, the EML is slightly increased with the core diameters from D_{core} = 280 µm to D_{core} = 440 µm for three porosities for such as 66%, 76%, and 86%. At 1 THz frequency of optimum parameters for 86%, 76%, and 66% porosities and optimum core diameter D_{core} = 420 µm, EML is calculated 0.0079 cm^{-1}.

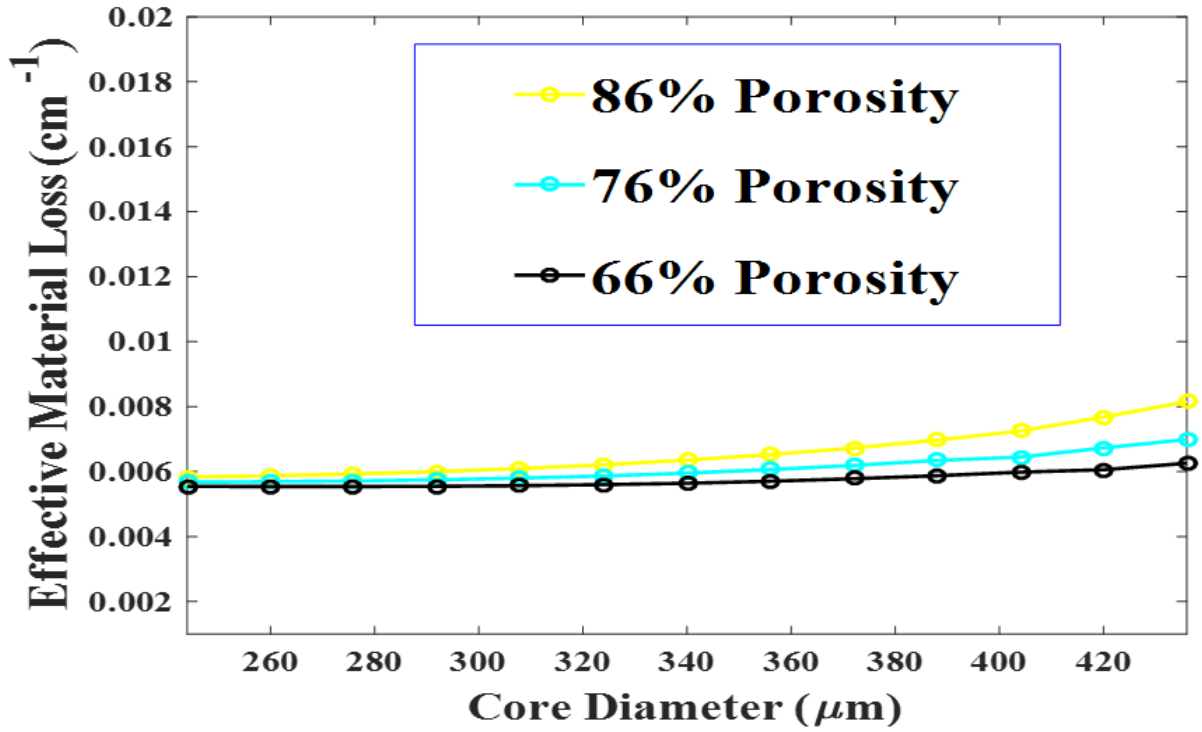

Figure 5: Presentation of EML with the core diameters.

Figure 6 displays that the PF of the core, cladding, and materials has good relationships with frequency ranges ranging from 0.80 to 3 THz. The majority of the light passes through the core area, while some power is lost in the cladding and materials areas. At 1 THz frequency, optimum parameters and core diameter D_{core} = 420 µm, 85%, 0.25%, and 21% values are the core, cladding, and materials of the power fraction.

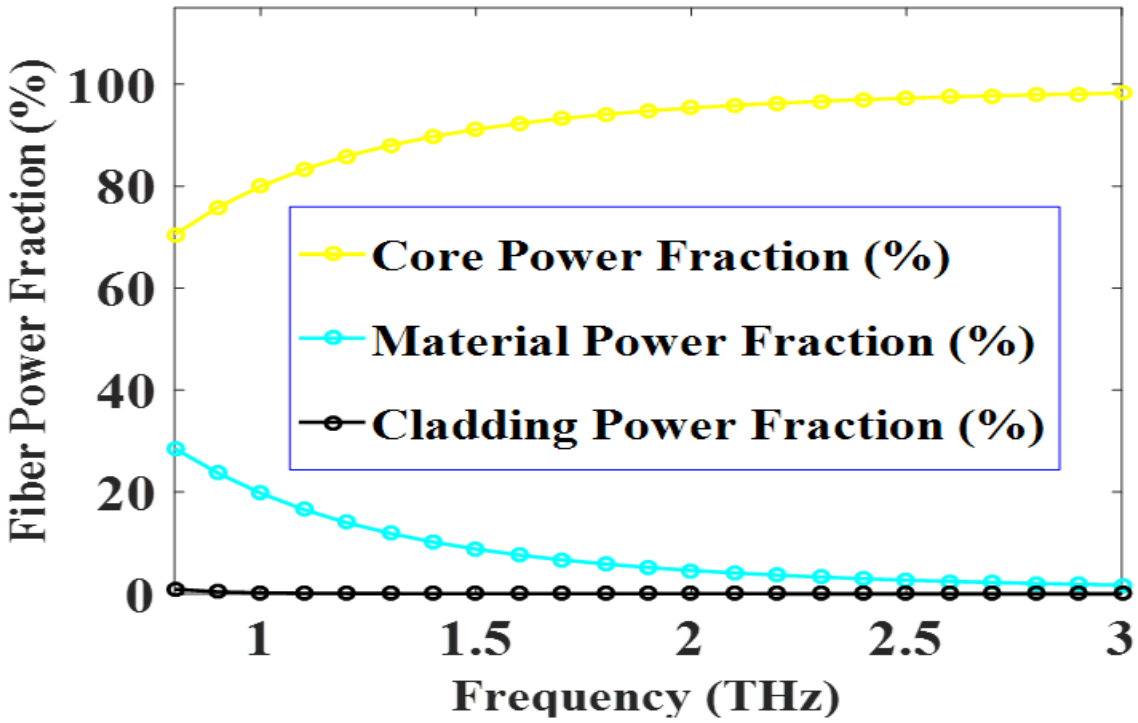

Figure 6: Core power with respect to the frequencies.

In Figure 7, the SL is slightly growing with the frequency ranges from 0.80 to 3 THz. For 86% porosity and 1 THz frequency, the SL is at 1.27×10^{-10} dB/km.

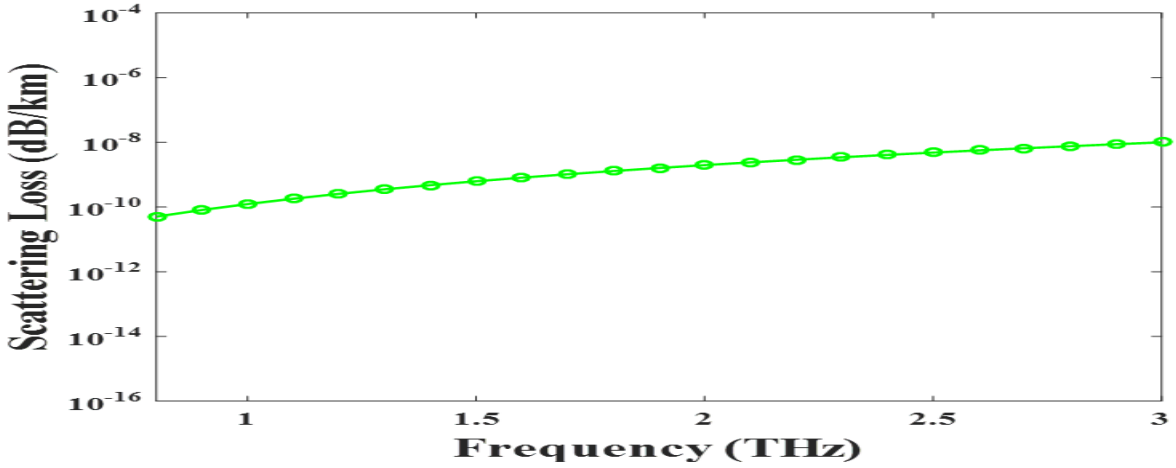

Figure 7: Graphical representation of scattering loss with respect to the frequencies.

In Figure 8, the confinement loss (CL) is decreasing with the frequency ranges from 0.80 to 3 THz. For 86% porosity and 1 THz frequency, confinement loss (CL) is the order of 3.35×10^{-16} dB/m.

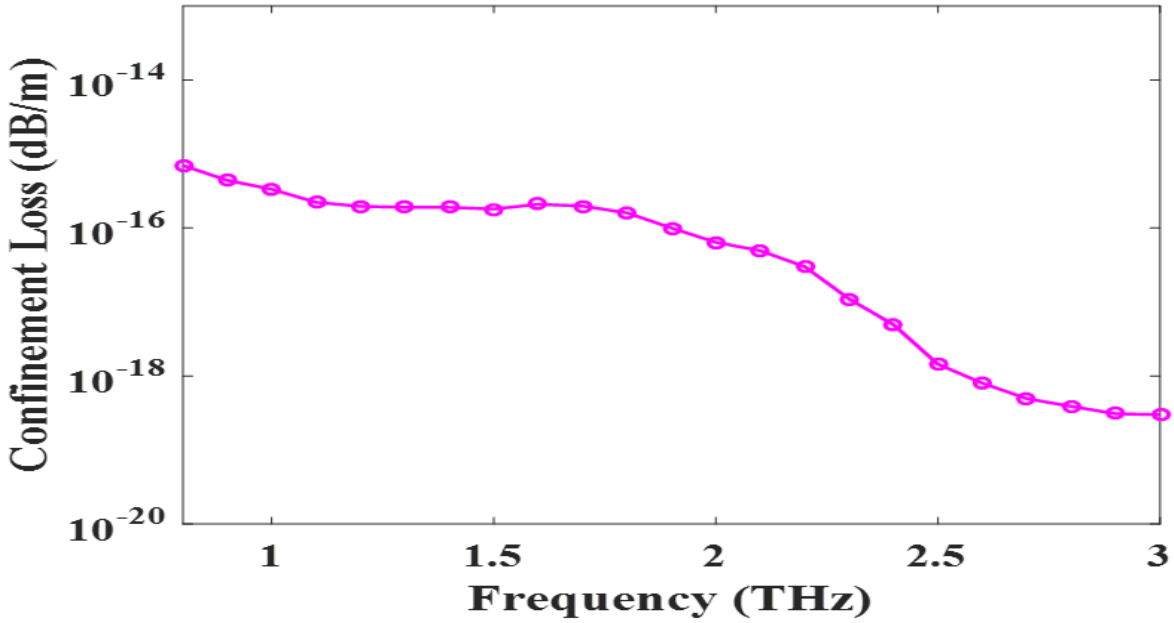

Figure 8: Presentation of CL along with the frequencies.

In this graphical Figure 9, the V-parameter is increasing from 0.80 to 3 THz and this V-parameter shows single mood communication system ($V-\text{parameter} \leq 2.045$). Here, the optimum cladding diameter is 282 µm, cladding pitch of 345 µm, diameter of core d_a = 70 µm ,d_b= 160 µm and core pitch Λ_c=100 µm.

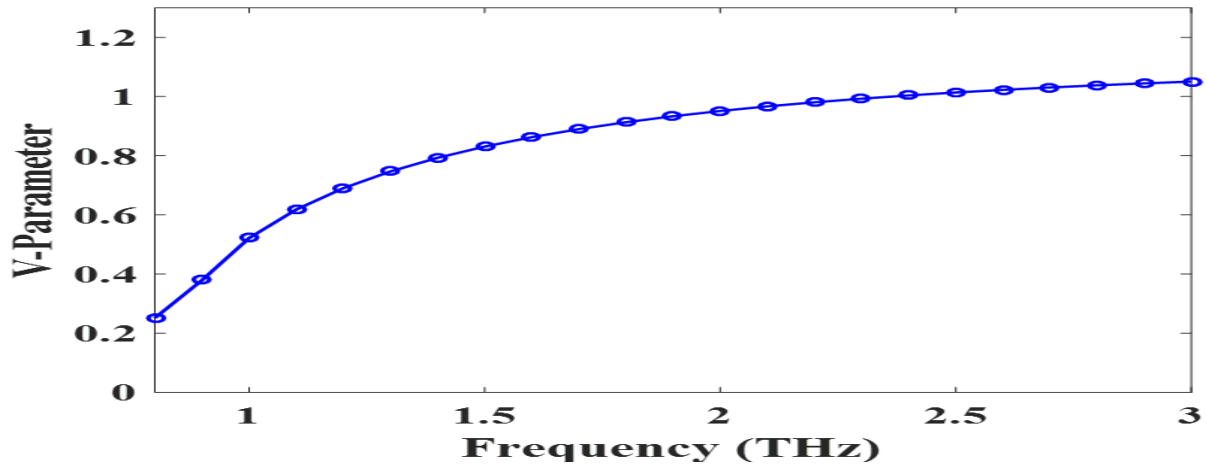

Figure 9: Calculation of V-parameter along with the frequencies.

In Table 1, the projected D-PCF has EML is 0.0079 cm^{-1}, a larger EA of 3.49×10^{-8} m^2, CPF of 85 percent, and a low CL of 3.35×10^{-16} dB/m than other proposed PCFs.

Table 1: optical properties among the proposed D-PCF and other proposed PCFs.

Ref.	EML (cm^{-1})	Porosity (%)	Power Fraction	Confinement Loss (dB/m)	Effective Area (A_{eff} (m^2))
[33]	0.047	-	54%	-	2.42×10^{-07}
[34]	0.081	-	46.9%	1.96×10^{-03}	1.24×10^{-03}
[35]	0.1	-	57.50%	1.38×10^{-12}	1.1×10^{-05}
[36]	0.038	74	56%	2.35×10^{-01}	6.75×10^{-05}
[37]	0.110	-	-	-	0.98×10^{-07}
Proposed D-PCF	0.0079	86	85%	3.35×10^{-16}	3.49×10^{-8}

Here, fabrication is an important way to fabricate the photonic crystal fiber. Much fabrication technique such as stack and draw, tube stacking drilling, sol-gel [38–42] but the sol-gel [43] process will be appropriate to manufacture the proposed D-PCF.

Conclusion

In this study, a decagonal (D-PCF) photonic crystal fiber was examined using PML and the FEM based COMSOL Multiphysics software tool for communication network performance analysis. In addition, we used ZEONEX as a background material to remove EML, CL, and SL. After reviewing all of the graphical results, we discovered that our D-PCF has an EML, a large effective area, a core power fraction, and a low CL and SL of 0.0079 cm^{-1}, 3.49×10^{-8} m^2, 85%, 3.35×10^{-16} dB/m and 1.27×10^{-10} dB/km correspondingly at 1 THz frequency range. So, our D-PCF is proper for communication parts in the THz regions.

Competing Interests: The authors declare that they have no competing of interest.

Acknowledgement: The authors are grateful to the participants who contributed to this research. The authors have not received any funding for this research.

References:

[1] M. I. Islam, K. Ahmed, S. Asaduzzaman, B. K. Paul, T. Bhuiyan, S. Sen, M. S. Islam, and S. Chowdhury : Design of single mode spiral photonic crystal fiber for gas sensing applications. Sensing and Bio-Sensing Research, 13 , 55-62, (2017).

[2] Islam, M.I., Ahmed, K., Sen, S., Chowdhury, S., Paul, B.K., Islam, M.S., Asaduzzaman, S.: Design and optimization of photonic crystal fiber-based sensor for gas condensate and air pollution monitoring. Photonic Sens 7(3), 234–245 (2017).

[3] M. S. Hossain, S. Sen, and M. M. Hossain: Performance analysis of octagonal photonic crystal fiber (O-PCF) for various communication applications: Phys. Scr., 96(5), 55506 (2021) doi: 10.1088/1402-4896/abe323.

[4] Pinto, D., Obayya, S.S.A.: Improved complex envelope alternative direction implicit finite difference time domain method for photonic bandgap cavities. IEEE J. Lightwave Technol. 25(1), 440–447 (2007).

[5] M. Nagel, P. H. Bolivar, M. Brucherseifer, H. Kurz, A. Bosserhoff, and R. Büttner: Integrated THz technology for label-free geneticdiagnostics. Appl. Phys. Lett., 80 (1), 154–156 (2002).

[6] Vigneswaran, D., Ayyanar, N., Sharma, M., Sumathi, M., Rajan, M., Porsezian, K.: Salinity sensor using photonic crystal fber. Sens. Actuators A Phys. 269, 22–28 (2018).

[7] Amiri, I.S.; Paul, B.K.; Ahmed, K.; Aly, A.H.; Zakaria, R.; Yupapin, P.; Vigneswaran, D.: Tri-core photonic crystal fiber based refractive index dual sensor for salinity and temperature detection. Microw. Opt. Technol. Lett. (2018).

[8] Md. Selim Hossain, M.M. Kamruzzaman, Shuvo Sen, Mir Mohammad Azad and Mohammad Sarwar Hossain Mollah, Hexahedron core with sensor based photonic crystal fiber: An approach of design and performance analysis", Sensing and Bio-Sensing Research,2021, doi: https://doi.org/10.1016/j.sbsr.2021.100426

[9] S. Islam, S. Rana, M. R. Islam, M. Faisal, H. Rahman, and J. Sultana : Porous core photonic crystal fiber for ultra-low material loss in THz regime. IET Commun., 10(16), 2179–2183, (2016).

[10] Wang, K., Mittleman, D.M.: Metal wires for terahertz waveguiding. Nature 432, 376–379 (2004).

[11] Bowden, B., Harrington, J.A., Mitrofanov, O.: Silver/polystyrenecoated hollow glass waveguides for the transmission of terahertz radiation. Opt. Lett. 32(20), 2945–2947(2007)

[12] Skorobogatiy, M., Dupuis, A.: Ferroelectric all-polymer hollow Bragg fibers for terahertz guidance. Appl. Phys. Lett. 90(11),113514 (2007).

[13] Jeon, T. I., Zhang, J., and Grischkowsky, D : THz Somerfeld wave propagation on a single metal wire. Applied Phys. Lett., 86(16), 161904, (2005).

[14] Hassani, A., Dupuis, A., Skorobogatiy, M.: Porous polymer fibers for low-loss terahertz guiding. Opt. Express 16(9), 6340–6351(2008)

[15] Chen, L., Chen, H., Kao, T., Lu, J., Sun, C.: Low-loss subwavelength plastic fiber for terahertz wave guiding. Opt. Lett. 31(3), 308–310 (2006)

[16] X. Tang, Y. Jiang, B. Sun, J. Chen, X. Zhu, P. Zhou, D. Wu, and Y. Shi, IEEE Photonics Technology Letters 25, 331 (2013).

[17] W. Yuan, L. Khan, D. J. Webb, K. Kalli, H. K. Rasmussen, A. Stefani, O. Bang : Humidity insensitive TOPAS polymer ber Bragg grating sensor. Opt. Express, 19(20) , 19731–19739 (2011).

[18] Bulbul, Abdullah A.-M.; Imam, Farjana; Awal, Md. A.; Mahmud, M. A.P.: A Novel Ultra-Low Loss Rectangle-Based Porous-Core PCF for Efficient THz Waveguidance: Design and Numerical Analysis. Sensors , 20(22), 6500 (2020).

[19] M. S. Hossain, M. M. Hasan, S. Sen, M. S. H. Mollah, and M. M. Azad: Simulation and analysis of ultra-low material loss of single-mode photonic crystal fiber in terahertz (THz) spectrum for communication applications. J. Opt. Commun., 4873,(2021) doi: 10.1515/joc-2020-0224.

[20] X. Jiang, N. Y. Joly, M. A. Finger, F. Babic, G. K. Wong, J. C. Travers, P. S. J. Russell: Deep-ultraviolet to mid-infrared super continuum generated in solidcore ZBLAN photonic crystal fiber. Nat. Photonics, 9(2), 133–139 (2015).

[21] Dash, J.N., Jha, R.: Graphene-based birefringent photonic crystal fber sensor using surface plasmon resonance. IEEE Photon. Technol. Lett. 26(11), 1092–1095 (2014)

[22] Hossain, M.S., Sikder, A.S., Sen, S. et al. Design and numerical analysis of Zeonex-based photonic crystal fiber for application in different types of communication networks. J Comput Electron (2021). https://doi.org/10.1007/s10825-021-01704-9

[23] Hasanuzzaman GKM, Habib MS, Razzak SA, Hossain MA, Namihira Y. Low loss single-mode porous-core kagome photonic crystal fiber for THz wave guidance. J Light Tech 2015;33(19):4027–31.

[24] Hasan MR, Islam MA, Rifat AA. A single mode porous-core square lattice photonic crystal fiber for THz wave propagation. J Eur Opt Soc-Rap Pub 2016;12(1):15.

[25] Islam MS, Rana S, Islam MR, Faisal M, Rahman H, Sultana J. Porous core photonic crystal fibre for ultra-low material loss in THz regime. IET Com 2016;10(16):2179–83.

[26] Sen S, Islam MS, Paul BK, Islam MI, Chowdhury S, Ahmed K, et al. Ultra-low loss with single mode polymer-based photonic crystal fiber for THz waveguide. J Opt Com 2017. https://doi.org/10.1515/joc-2017-0104.

[27] Ren, Hai Zhen, Peng Guo, and Lin Feng Yang. The Numerical Calculation on the Effective Area of Photonic Crystal Fiber Using FEM, Advanced Materials Research 468471 (February 2012): 24172422. doi: 10.4028/www.scientific.net/amr.468-471.2417.

[28] Luo J., Tian F., Qu H., Li L., Zhang J., Yang X., Yuan L. Design and numerical analysis of a THz square porous-core photonic crystal fiber for low flattened dispersion, ultrahigh birefringence. Appl. Opt. 2017; 56:6993–7001. doi: 10.1364/AO.56.006993.

[29] Islam R, Habib MS, Hasanuzzaman GKM, Rana S, Sadath MA, Markos C (2016) A novel low-loss diamond-core porous fiber for polarization maintaining terahertz transmission. IEEE Photon Technol Lett 28(14):1537–1540.

[30] Islam M.S., Sultana J., Rana S., Islam M.R., Faisal M., Kaijage S.F., Abbott D. Extremely low material loss and dispersion flattened TOPAS based circular porous fiber for long distance terahertz wave transmission. Opt. Fiber Technol. 2017; 34:6–11. doi: 10.1016/j.yofte.2016.11.014.

[31] Ahmed K, Chowdhury S, Paul BK, Islam MS, Sen S, Islam MI, et al. Ultrahigh birefringence, ultralow material loss porous core single-mode fiber for terahertz wave guidance. Appl Opt 2017;56(12):3477–3483. DOI:10.1364/AO.56.003477.

[32] Rana S, Hasanuzzaman GK, Habib S, Kaijage SF, Islam R. Proposal for a low loss porous core octagonal photonic crystal fiber for T-ray wave guiding. Opt Eng. 53(11):115107–115107. DOI:10.1117/1.OE.53.11.115107(2014)

[33] K. Ahmed, M. Islam, S. Sen, B.K. Paul, S. Chowdhury, M. Hasan, M.S. Uddin, S. Asaduzzaman, A.N. Bahar, Low-loss single mode terahertz microstructure fiber with near-zero-flattened dispersion, Advanced Science, Engineering and Medicine 9 (10) (2017) 829–836.

[34] J. Luo, F. Tian, H. Qu, L. Li, J. Zhang, X. Yang, L. Yuan, Design and numerical analysis of a THz square porous-core photonic crystal fiber for low flattened dispersion, ultrahigh birefringence, Appl. Opt. 56 (2017) 6993–7001.

[35] B.K. Paul, M. Haque, K. Ahmed, S. Sen, A novel hexahedron photonic crystal fiber in terahertz propagation: design and analysis, Photon. 6 (2019) 32–38.

[36] Paul BK, Ahmed K (2020) Analysis of terahertz waveguide properties of Q-PCF based on FEM scheme. Opt Mater 100:109634.

[37] Islam R, Habib MS, Hasanuzzaman GKM, Rana S, Sadath MA, Markos C (2016) A novel low-loss diamond-core porous fiber for polarization maintaining terahertz transmission. IEEE Photon Technol Lett 28(14):1537–1540.

[38] Paul BK, Bhuiyan T, Abdulrazak LF, Sarker K, Hassan MM, Shariful S, Ahmed K (2019) extremely low loss optical waveguide for terahertz pulse guidance. Results in Physics 15:102666.

[39] Ahmed K, Chowdhury S, Paul BK, Islam MS, Sen S, Islam MI, et al. Ultrahigh birefringence, ultralow material loss porous core single-mode fiber for terahertz wave guidance. Appl Opt 2017;56(12):3477–3483. DOI:10.1364/AO.56.003477.

[40] Rana S, Hasanuzzaman GK, Habib S, Kaijage SF, Islam R. Proposal for a low loss porous core octagonal photonic crystal fiber for T-ray wave guiding. Opt Eng. 53(11):115107–115107. DOI:10.1117/1.OE.53.11.115107(2014)

[41] Islam, M.S., Sultana, J., Atai, J., Abbott, D.,Rana, S., Islam, M.R.: Ultra lowloss hybrid core porous fiber for broadband applications. Appl. Opt. 56(9), 1232–1237 (2017)

[42] Tang, X., Jiang, Y., Sun, B., Chen, J., Zhu, X., Zhou, P., Wu, D., Shi,Y.: Elliptical hollow fiber with inner silver coating for linearly polarized terahertz transmission. IEEE Photonics Technol. Lett. 25(4), 331–334 (2013)

[43] El Hamzaoui, H., Ouerdane, Y., Bigot, L., Bouwmans, G., Capoen, B., Boukenter, A., Girard, S. and Bouazaoui, M., Sol-gel derived ionic copper-doped microstructured optical fiber: a potential selective ultraviolet radiation dosimeter. Optics express, 20(28), pp.29751-29760, (2012).